Chapter 11
Development of a Bi-fuel SI Engine Model

K. Rezapour

Abstract Natural gas is a promising alternative fuel, with the potential to meet strict engine emission regulation, and is cheaper than other fuels in many countries. Use of natural gas as an automotive fuel may bring a reduction of environmental pollutants and reduce the economic costs of the transportation sector. As an intermediate step, and an alternative to dedicated CNG engines bi-fuel engines, powered by gasoline and compressed natural gas (CNG), provide many an opportunity. In support of the development of such engines and to aid analysis and improvement in this study, a four-stroke bi-fuel spark ignition (SI) engine model is developed. The engine model is based on the two-zone combustion model, and it has the ability to simulate turbulent combustion and compared to computational fluid dynamic (CFD) models it is computationally faster and efficient. The selective outputs are cylinder temperature and pressure, heat transfer, brake work, brake thermal and volumetric efficiency, brake torque, brake power (BP), brake-specific fuel consumption (BSFC), brake mean effective pressure (BMEP), concentration of CO_2, brake-specific CO (BSCO) and brake-specific NO_x ($BSNO_x$). In this research, the effect of engine speed, equivalence ratio and performance parameters using gasoline and CNG fuels are analysed. In addition, the model has been validated by experimental data using the results obtained from bi-fuel engine tests. Therefore, this engine model is capable for prediction, analysis and useful for optimisation of the engine performance parameters and minimisation of the emissions. In addition, in this chapter, a specific bi-fuel engine is studied and discussed that is used in the vast majority (almost are taxi). Therefore, the model and its results are significant.

Keywords Bi-fuel • Engine performance • Emissions • Engine modelling

K. Rezapour (✉)
Department of Mechanical Engineering, Faculty of Engineering, Islamic Azad University, Karaj Branch, Alborz, Iran
e-mail: rezapour@kiau.ac.ir

I. Dincer et al. (eds.), *Progress in Clean Energy, Volume 2*,
DOI 10.1007/978-3-319-17031-2_11

Nomenclature

A	Area exposed to heat transfer (m^2)
aBDC	After BDC
aTDC	After TDC
b	Bore of cylinder (m)
bBDC	Before BDC
bTDC	Before TDC
C_p	Specific heat at constant pressure (J kg^{-1} k^{-1})
C_b	Blow by coefficient (s^{-1})
E	Total energy (J)
EVO	Exhaust valve opening
H	Enthalpy (J)
h	Specific enthalpy (J kg^{-1})
h	Heat transfer coefficient (W m^{-2} K^{-1})
IVC	Inlet valve closing
m	Mass (kg)
P	Pressure (Pa)
PPM	Particle per million
Q	Heat transfer (J)
r	Compression ratio
R	Gas constant
RON	Research octane number
s	Specific entropy (J kg^{-1} K^{-1})
T	Temperature (K)
u_p	Engine piston speed (m/s)
V	Volume (m^3)
W	Work done (J)
WOT	Wide open throttle
x	Burnt mass fraction

Greek Letters

v	Specific volume (m^3 kg^{-1})
θ	Crank angle (°CA)
θ_0	Start of combustion (°CA)
$\Delta\theta$	Total combustion duration (°CA)
ω	Angular velocity (rad s^{-1})
ϕ	Equivalence ratio
φ_{ed}	Charge-up efficiency
γ_r	Mole fraction

11.1 Introduction

The Kyoto protocol called for reduction in greenhouse gas emissions between 2008 and 2012 to levels that are 5.2 % below 1990 levels in 38 industrialised countries [1]. Additionally, ever-increasing oil prices and security of supply issues are focussing attentions on alternative sources of motive energy. Consequently, vehicle manufacturers are focussing their interests on a diversity of engine technologies. This includes the development of engines that are capable of making use of alternative fuels such as CNG. CNG consists of 88 % methane and may be used in either CNG or liquefied gas forms in vehicle. CNG is cheaper and cleaner than gasoline but it reduces the engine brake power [2].

With regard to the climatic situation of some countries, and considering the existence of broad networks of gas distribution, natural gas can be a suitable alternative to conventional fuels. The bi-fuel vehicle in some countries, along with the implementation of strategies for the gasification of vehicles, has been identified, i.e., workshop conversion of vehicle in move (short-term approach), factory production of bi-fuel engines (midterm approach) and designing and producing base CNG engine (long-term approach) [2]. Therefore, developing bi-fuel engines (gasoline and CNG) in the short and midterm is a strategy for achieving this important aim. A major support for better achievement of this subject is applied studies for analysis and improvement of the engine performance.

Many studies and experimental works have been undertaken on CNG-fuelled engines; for example, Lapetz et al. [3] developed a Ford compressed natural gas bi-fuel truck. To ensure safety and control emissions, they modified the base vehicle's specification for conversion to operation of bi-fuel CNG. Flame speed in natural gas is lower than gasoline. For this reason, the duration of the total combustion is to extend compared with gasoline and diesel [4]. Zuo and Zhao [5] developed a QD model to analyse combustion process in SI pre-chamber natural gas engine. Evans and Blaszcsky [6] in their study characterising the performance and emissions of a bi-fuel Ricardo single-cylinder SI research engine showed a 12 % power and 5–50 % emission reduction when the engine is fuelled using natural gas. Further similar studies [7–9] have also been undertaken looking at CNG and related engine development. This chapter includes a model development and its experimental validation on a bi-fuel engine, as well as simulation results, discussion and conclusions.

11.2 Mathematical Model

The engine model developed herein is a quasi-dimensional, two-zone combustion model that solves the differential equations related to compression, combustion and expansion. Intake and exhaust processes computationally are calculated using an approximation method. In this model, the combustion chamber is divided into two

zones including an unburned mixture (zone 1) and burned mixture (zone 2). The distance between the two zones is the flame front. The flame is propagated turbulently and expanded in the combustion chamber over a spherical flame front:

$$\frac{\mathrm{d}E}{\mathrm{d}\theta} = \frac{\mathrm{d}Q}{\mathrm{d}\theta} - \frac{\mathrm{d}W}{\mathrm{d}\theta} + \sum_{\text{in}} \dot{m}h - \sum_{\text{out}} \dot{m}h \tag{11.1}$$

$$\frac{\mathrm{d}m}{\mathrm{d}\theta} = \sum_{\text{in}} \frac{\mathrm{d}m}{\mathrm{d}\theta} - \sum_{\text{out}} \frac{\mathrm{d}m}{\mathrm{d}\theta} \tag{11.2}$$

Equation (11.1) can be written as

$$\frac{\mathrm{d}(mu)}{\mathrm{d}\theta} = \frac{\mathrm{d}Q}{\mathrm{d}\theta} - p\frac{\mathrm{d}V}{\mathrm{d}\theta} + \sum_{\text{in}} h\frac{\mathrm{d}m}{\mathrm{d}\theta} - \sum_{\text{out}} h\frac{\mathrm{d}m}{\mathrm{d}\theta} \tag{11.3}$$

The thermodynamic properties are provided using the relations proposed by the following expressions [10] that are curve-fitted to the tabulated JANAF thermochemical tables [11]:

$$\frac{C_{P,i}}{R} = U_{i1} + U_{i2}T + U_{i3}T^2 + U_{i4}T^3 + U_{i5}T^4 \tag{11.4}$$

$$\frac{h_i}{RT} = U_{i1} + \frac{U_{i2}}{2}T + \frac{U_{i3}}{3}T^2 + \frac{U_{i4}}{4}T^3 + \frac{U_{i5}}{5}T^4 + \frac{U_{i6}}{T} \tag{11.5}$$

$$\frac{s_i}{R} = U_{i1}\ell nT + U_{i2}T + \frac{U_{i3}}{2}T^2 + \frac{U_{i4}}{3}T^3 + \frac{U_{i5}}{4}T^4 + U_{i7} \tag{11.6}$$

where C_p is the specific heat measured at a constant pressure, h is the specific enthalpy and s is the specific entropy. The coefficients U_{i1} to U_{i7} are calculated over two different temperature ranges [11], (1) $300 < T < 1{,}000$ K and (2) $1{,}000 < T < 5{,}000$ K.

When modelling with a single fuel, the equivalence ratio can be written as [12]

$$\phi = \left(\frac{\text{Fuel}}{\text{Air}}\right)_{\text{Act.}} \Big/ \left(\frac{\text{Fuel}}{\text{Air}}\right)_{\text{St.}} \tag{11.7}$$

where subscript Act. denotes the actual and St. denotes the stoichiometric air/fuel ratios.

The mass in a control volume may be calculated [12]

for $\theta_{\text{IVC}} \geq \theta \geq -360^\circ$ CA (intake)

$$m = \frac{V(\theta)}{\nu_u} \tag{11.8}$$

for $\theta_{\mathrm{EVO}} \geq \theta \geq \theta_{\mathrm{IVC}}$ (valve closed)

$$m = m_{\mathrm{IVC}} \exp[-C_b(\theta - \theta_{\mathrm{IVC}})/\omega] \tag{11.9}$$

for $360^\circ\,\mathrm{CA} \geq \theta \geq \theta_{\mathrm{EVO}}$ (blow down and exhaust)

$$m = \frac{V(\theta)}{\nu_b} \tag{11.10}$$

where subscripts b and u denote the burned gas and unburned gas regions, respectively. The cylinder volume is known at any crank angle, with compression ratio r, volume at TDC V_c (clearance volume) and $\varepsilon = \text{stroke}/2 \times \text{length of rod}$ [12]:

$$V(\theta) = V_c \left\{ 1 + \frac{r-1}{2} \left\{ 1 - \cos\theta + \frac{1}{\varepsilon} \left[1 - \left(1 - \varepsilon^2 \sin^2\theta \right)^{0.5} \right] \right\} \right\} \tag{11.11}$$

Here, the combustion model is the two-zone model that divides the combustion chamber into unburned and burned zone. These zones are distinct by a turbulent flame front that it is solved numerically. Therefore, the combustion parameters such as burned mass fraction ($x = m/m_{\mathrm{b}}$) combined into the model consist of laminar and turbulent flame speed.

The adiabatic flame temperature is the maximum temperature that the products of combustion will reach in the limiting case of no heat loss to the surroundings during the combustion process. The adiabatic flame temperature reaches its maximum value when complete combustion happens with the theoretical value of air. Recalling the definition of enthalpy [13], this can be stated as

$$H_{\mathrm{react}}(T_i, p) = H_{\mathrm{prod}}(T_{\mathrm{ad}}, p)$$

where subscript react denotes reactants and prod denotes products, T_{ad} is the adiabatic flame temperature and T_i is the initial flame temperature.

The laminar flame with gasoline and CNG (methane) fuels, according to Metghalchi and Keck [14], is calculated as follows:

$$u_L = u_{L,0} \left(\frac{T_u}{T_0} \right)^{\alpha} \left(\frac{P}{P_0} \right)^{\beta} \left(1 - 2.0 x_b{}^{0.77} \right) \tag{11.12}$$

in which P is the pressure and T_u is the unburned zone temperature. $T_0 = 298\,K$ and $P_0 = 1(\mathrm{atm})$ are the reference temperature and pressure; α, β and $u_{L,0}$ are constants and x_b is the mole fraction of the residual gas in the unburned mixture. These constants are defined as follows for gasoline fuels:

$$\alpha = 2.18 - 0.8(\phi - 1)$$
$$\beta = -0.16 + 0.22(\phi - 1)$$
$$u_{L,0} = 0.305 - 0.549(\phi - 1.21)^2$$

The flame speed of the natural gas and air mixture has been calculated using the relations presented by Gu et al. [15]. This relation is

$$u_L = u_{L,0}\left(\frac{T_u}{T_0}\right)^{\gamma}\left(\frac{P_u}{P_0}\right)^{\kappa} \tag{11.13}$$

γ and κ depend on ϕ. They have determined the quantities with a non-significant error (0.014 %) for different quantities as shown below:

$$u_L = \begin{cases} 0.314\left(\frac{T_u}{T_0}\right)^{2.000}\left(\frac{P_u}{P_0}\right)^{-0.438} & \phi = 1.2 \\ 0.36\left(\frac{T_u}{T_0}\right)^{1.162}\left(\frac{P_u}{P_0}\right)^{-.0374} & \phi = 1.0 \\ 0.259\left(\frac{T_u}{T_0}\right)^{2.105}\left(\frac{P_u}{P_0}\right)^{-0.504} & \phi = 0.8 \end{cases} \tag{11.14}$$

There are different methods that may be used for the calculation of the turbulent flame speed. In this chapter, the Damkohler method [16] has been used to calculate the turbulent flame speed:

$$u_t = u^{'} + u_L \tag{11.15}$$

$$u^{'} = 0.75\overline{u_p}\left(1 - 0.5\frac{\theta - 360}{45}\right) \tag{11.16}$$

In the above relations, θ is the crank angle at the end of the compression stroke, which is equal to 360 degrees. In addition, u_p is the engine piston speed.

Burned mass amount during the combustion can be determined using the relation as follows [17]:

$$\frac{\mathrm{d}m_b}{\mathrm{d}\theta} = A_f.\rho_u.u_L.\left(1 + \frac{u_t}{u_L}\right)/6N \tag{11.17}$$

$$A_f = 4\pi R_f^2 \tag{11.18}$$

$$R_f = \left(\frac{3V_b}{4\pi}\right)^{\frac{1}{3}} \tag{11.19}$$

where N is the engine speed in rad/s, ρu is the unburned mass density (g/m^3), Af is the flame front area (m^2) and R_f is the radius of flame (m).

Under the atmospheric air composition assumption (79 %V nitrogen and 21 %V oxygen), and conditioned $\phi < 3$, the species including O, H, OH and NO are important due to dissociation [12]. Therefore, the combustion reaction becomes

$$\begin{aligned} &\varepsilon\phi C_\alpha H_\beta O_y N_\delta + 0.21O_2 + 0.79N_2 \rightarrow \\ &x_1 CO_2 + x_2 H_2O + x_3 N_2 + x_4 O_2 + x_5 CO \\ &+ x_6 H_2 + x_7 H + x_8 O + x_9 OH + x_{10} NO \end{aligned} \tag{11.20}$$

x_1 to x_{10} represent the products' mole fractions. Moreover, with two additional mole fractions in the products including N and Ar, which they [18] are made preparation content user specified air quality, and Depcik [19] improved the Olikara and Borman model. In terms of heat loss, heat transfer model is expressed [12]:

$$\frac{dQ}{d\theta} = \frac{-\dot{Q}_{loss}}{\omega} = \frac{-\dot{Q}_b - \dot{Q}_u}{\omega} \tag{11.21}$$

with

$$\dot{Q}_b = h \sum_{i=h,\ p,\ \ell} A_{bi}(T_b - T_{wi}) \tag{11.22}$$

$$\dot{Q}_u = h \sum_{i=h,\ p,\ \ell} A_{ui}(T_u - T_{wi}) \tag{11.23}$$

where A_{bi} and A_{ui} are the burned and unburned gas areas in heat transfer model in contact at temperature T_{wi} with the combustion chamber component, x is the mass fraction burned and subscripts h, p and ℓ denote the cylinder head, piston crown and linear, respectively. The following relations are [12]:

$$A_{bi} = A_i x^{0.5} \tag{11.24}$$

$$A_{ui} = A_i\left(1 - x^{0.5}\right) \tag{11.25}$$

Here, $A_i = A_h + A_\ell$, and are determined by $A_h = \frac{\pi b^2}{2}$ (hemispherical cylinder head), $A_p = \frac{\pi b^2}{4}$ (flat piston crown) and $A_\ell = \frac{4V(\theta)}{b}$ (linear surface area exposed to gases).

The heat transfer rate is calculated using the following equation from Woschni [20]:

$$\dot{Q} = A_w\left(c.b^{-0.2}P^{0.8}.T^{-0.55}.u^{0.8}\right).(T_w - T) \tag{11.26}$$

In this equation, the speed u is determined from

Table 11.1 Woschni's formula parameters [20]

Gas exchange	$c_1 = 6.18$	$c_2 = 0$
Compression	$c_1 = 2.28$	$c_2 = 0$
Combustion and expansion	$c_1 = 2.28$	$c_2 = 3.24\text{E-}3$

$$u = c_1 u_p + c_2 \frac{V.T_r}{P_r.V_r}(P - P_m) \tag{11.27}$$

where

$$u_p = 2LN \tag{11.28}$$

The parameters P_r, T_r and V_r are evaluated at any reference condition, such as inlet valve closure. In addition, A_w, P_m, L and N are cylinder wall area, motoring pressure, piston stroke and engine speed, respectively. The values for c_1 and c_2 suggested by Woschni are listed in Table 11.1.

By solving the equations of energy conversion for each stage, the pressure and temperature rate changes can be calculated [12]:

$$\frac{\mathrm{d}T_b}{\mathrm{d}\theta} = \frac{-h \sum_{i=h,\,p,\,\ell} A_{ui}(T_b - T_{wi})}{m\omega c_{p_b}} + \frac{v_b}{C_{p_b}} \frac{\partial \ell n v_b}{\partial \ell n T_b} \frac{\mathrm{d}p}{\mathrm{d}\theta} + \frac{h_u - h_b}{x c_{p_b}} \left[\frac{\mathrm{d}x}{\mathrm{d}\theta} - \left(x - x^2\right) \frac{C_b}{\omega} \right] \tag{11.29}$$

$$\frac{\mathrm{d}T_u}{\mathrm{d}\theta} = \frac{-h \sum_{i=h,\,p,\,\ell} A_{ui}(T_u - T_{wi})}{m\omega c_{p_u}(1 - x)} + \frac{v_u}{C_{p_u}} \frac{\partial \ell n v_u}{\partial \ell n T_u} \frac{\mathrm{d}p}{\mathrm{d}\theta} \tag{11.30}$$

$$\frac{\mathrm{d}p}{\mathrm{d}\theta} = \frac{A + B + C}{D + E} \tag{11.31}$$

where

$$A = \frac{1}{m}\left(\frac{\mathrm{d}V}{\mathrm{d}\theta} + \frac{VC_b}{\omega}\right) \tag{11.32}$$

$$B = \frac{h}{m\omega}\left[\frac{v_b}{c_{p_b}} \frac{\partial \ell n v_b}{\partial \ell n T_b} \frac{\sum_{i=h,\,p,\,\ell} A_{bi}(T_b - T_{wi})}{T_b} + \frac{v_u}{c_{p_u}} \frac{\partial \ell n v_u}{\partial \ell n T_u} \frac{\sum_{i=h,\,p,\,\ell} A_{ui}(T_u - T_{wi})}{T_u} \right] \tag{11.33}$$

$$C = -(v_b - v_u)\frac{\mathrm{d}x}{\mathrm{d}\theta} - v_b \frac{\partial \ell n v_b}{\partial \ell n T_b}\frac{h_u - h_b}{c_{p_b} T_b}\left[\frac{\mathrm{d}x}{\mathrm{d}\theta} - \left(x - x^2\right)\frac{C_b}{\omega}\right] \tag{11.34}$$

$$D = x\left[\frac{v_b^2}{c_{p_b} T_b}\left(\frac{\partial \ell n v_b}{\partial \ell n T_b}\right)^2 + \frac{v_b}{p}\frac{\partial \ell n v_b}{\partial \ell n p}\right] \tag{11.35}$$

$$E = (1 - x)\left[\frac{v_u^2}{c_{p_u} T_u}\left(\frac{\partial \ell n v_u}{\partial \ell n T_u}\right)^2 + \frac{v_u}{p}\frac{\partial \ell n v_u}{\partial \ell n p}\right] \tag{11.36}$$

Equations (11.29)–(11.36) are functions of θ, p, T_b and T_u and have been solved using a fourth-order Runge-Kutta solver. A detailed solution procedure of the quasi-dimensional combustion model is shown in Fig. 11.1.

Intake and exhaust processes computationally are calculated using an approximation method [21]. In this method, pressure loss is determined during the intake process by the Bernoulli equation for one-dimensional incompressible flow. In addition, intake pressure and temperature, exhaust pressure and temperature and volumetric efficiency are determined as

$$p_i = p_0 - \Delta p_i \tag{11.37}$$

$$T_i = (T_0 + \Delta T + \gamma_r T_e)/(1 + \gamma_r) \tag{11.38}$$

$$p_e = (1.05 \div 1.25)\, p_0 \tag{11.39}$$

$$T_e = T_b/(p_b/p_e)^{1/3} \tag{11.40}$$

$$\eta_v = \varphi_{\mathrm{ed}}[r/(r-1)](p_i/p_0)[T_0/(T_0 + \Delta T + \gamma_r T_e)] \tag{11.41}$$

p_i, Δp_i, T_i, p_e, T_e, T_b, P_b, f, φ_{ed} and η_v are intake pressure, pressure loss (manifold), intake temperature, exhaust pressure and temperature, burned temperature and pressure, mole fraction, charge-up efficiency and volumetric efficiency, respectively.

Therefore, simulation and modelling of pressure, temperature, work and heat transfer are possible for the bi-fuel four-stroke SI engine running on gasoline and CNG fuels. The solution procedure of the quasi-dimensional combustion model is shown in Fig. 11.1.

The total friction work consists of three major components. These components are pumping work, rubbing friction work and accessory work. Data at WOT for several four-stroke cycle, four-cylinder SI engines, for providing total motored friction mean effective pressure (FMEP), as an engine speed function are adequately correlated by a relation as [22]

$$\mathrm{FMEP(bar)} = 0.97 + 0.15\left(\frac{N}{1,000}\right) + 0.05\left(\frac{N}{1,000}\right) \tag{11.42}$$

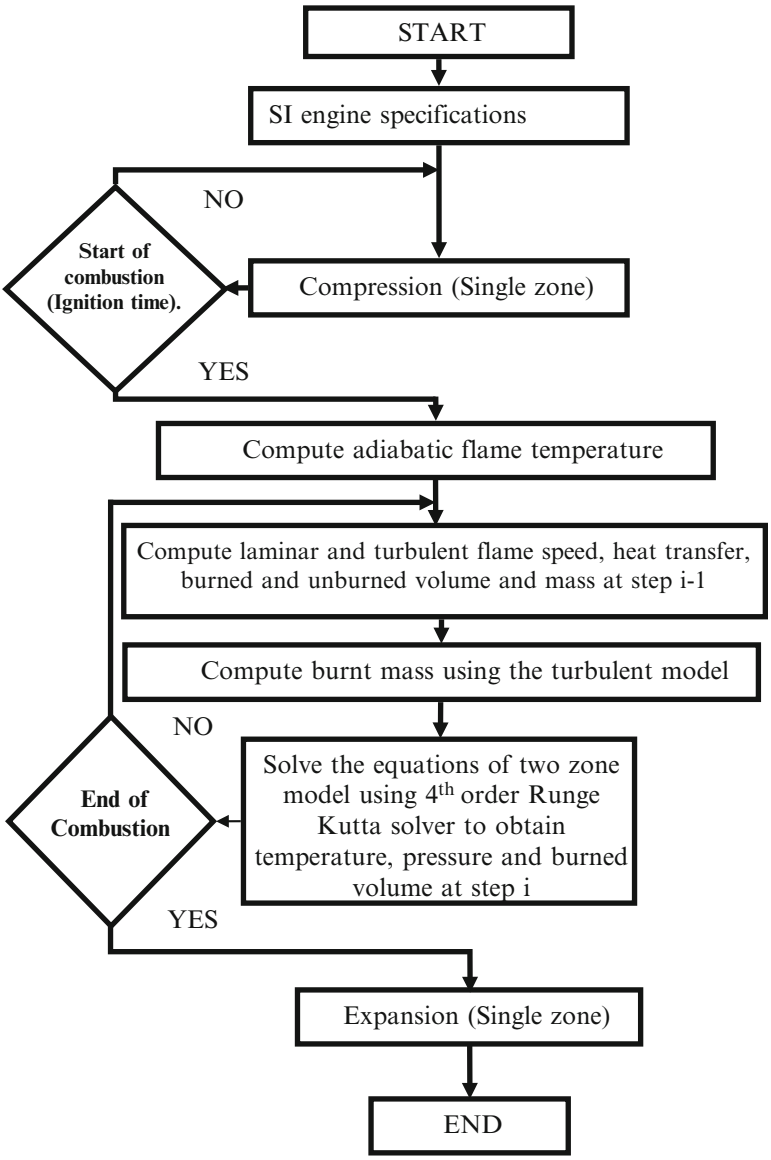

Fig. 11.1 Solution procedure of the quasi-dimensional combustion model

11.3 Model Validation

The model validation is undertaken through experimentation using the engine specified in Table 11.2. The engine is operated over its speed range, 1,500–6,000 r/min, at wide open throttle (WOT). Other experimental hardware include:

- Four-cylinder SI engine
- Eddy current dynamometer, Schenck WS230
- Exhaust gas analyser, Pierburg (HGA 400) 5 Gas Analyser
- Air fuel ratio device, Lambda Sensor Horiba (Mexa-700)
- CNG mass flow meters, Fisher Rosemount
- Gasoline mass flow metres, Maxmeter 214–410
- Cylinder Pressure device, Indimeter 619
- Data acquisition system, Ricardo
- Water and oil temperature control, Engine master software
- CNG storage

The engine and dynamometer specifications are listed in Tables 11.2 and 11.3. In addition, the layout of the test rig shows in Fig. 11.2. The test engine was a bi-fuel (gasoline and CNG) engine and prepared with an appropriate bi-fuelling system. Sensor applied for data gathering include an angle encoder, lambda, air mass flow metre, intake manifold, oil and fuel temperature and pressure, exhaust manifold, outlet water and oil thermocouples and intake manifold and oil pressure gauges. Data were gathered contemporaneously from the sensors and transfer to a data acquisition system. In addition, data for brake torque, brake power and exhaust gases was recorded, which included concentration of No_x, CO, CO_2, total-unburned hydrocarbon (THC) and O_2 in this study. In this model, CNG and gasoline have

Table 11.2 The engine specifications [23]

Engine type	Four-stroke, bi-fuel spark ignition
Fuel system	MPFI
Induction	Naturally aspirated
Number of cylinder	Four cylinder—In line
Bore (mm)	83
Stroke (mm)	81.4
Connecting rod (mm)	150.2
Displacement volume (cm^3)	1,761
Compression ratio	9.25
Maximum power	68.65 kW @ 6,000 rpm
Maximum torque	143 Nm @ 2,500 rpm
Inlet valve opening (IVO)	32° bTDC
Inlet valve closing (IVC)	64° aBDC
Exhaust valve opening (EVO)	59° bTDC
Exhaust valve closing (EVC)	17° aBDC

Table 11.3 Schenck dynamometer specifications

Dynamometer type	Schenck WS230
Maximum torque	750 (Nm)
Maximum speed	10,000 (rpm)
Maximum power	230 (kW)
Torsional spring	593 (Nm/rad × 1,000)
Weight	485 (kg)
Inertia	0.53 (kg/m^2)

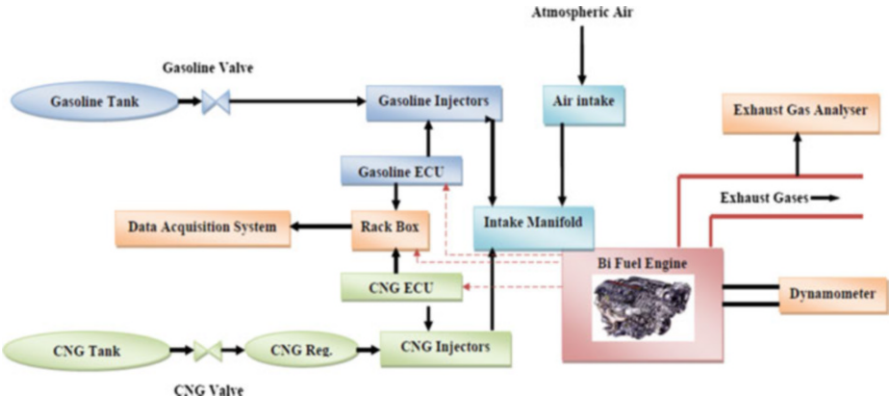

Fig. 11.2 A layout of test rig

been considered with composition of CH_4 and C_7H_{14} based on the properties and compositions of CNG and gasoline that are used in the tests [23], respectively.

For model validation, the experimental results are now compared. In running the model, the composition of CNG is taken as methane, CH_4 and gasoline, C_7H_{14} in accordance with the literature [23]. Model and experimental results such as brake power (BP), brake-specific CO (BSCO) and brake-specific NO_x ($BSNO_x$) are compared in Figs. 11.3, 11.4, 11.5, 11.6, 11.7 and 11.8. The results show good correspondence (with an average 8 % mean error). Therefore, the results support the fact that the model is valid for prediction of performance and emissions of the bi-fuel engine through the range tested.

11.4 Engine Thermodynamic Characteristics, Performance and Emissions

The validated model can be used to predict cylinder pressure, work done, heat transfer, brake thermal and volumetric efficiency, brake power (BP), brake mean effective pressure (BMEP), brake-specific fuel consumption (BSFC), equivalence

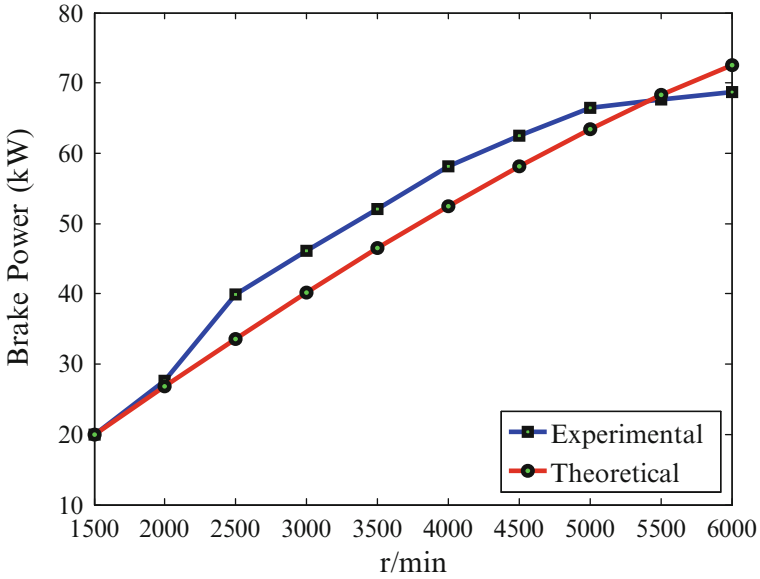

Fig. 11.3 A comparison of brake power results (gasoline)

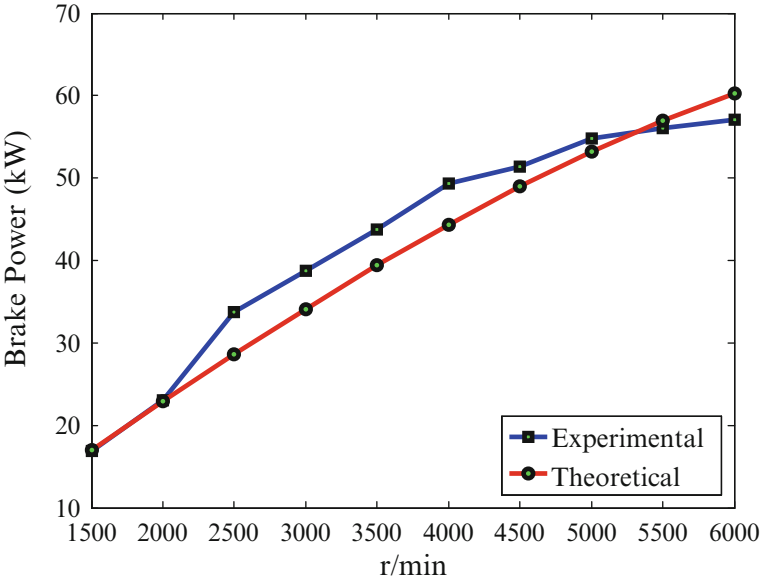

Fig. 11.4 A comparison of brake power results (CNG)

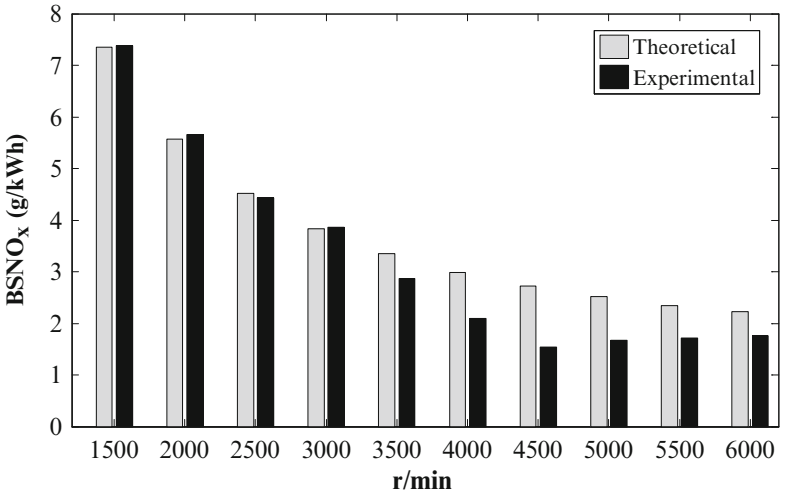

Fig. 11.5 Comparison of BSNO$_x$ results (gasoline)

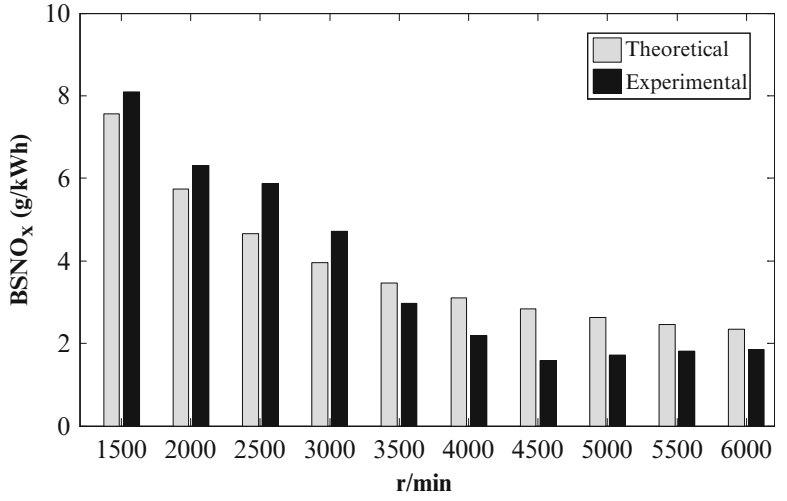

Fig. 11.6 Comparison of BSNO$_x$ results (CNG)

ratio and BSNO$_x$, BSCO and CO_2 concentration in exhaust gases. The engine performance and emissions for both fuels are now analysed and discussed.

In Figs. 11.9 and 11.10, cylinder pressure, work done for gasoline and CNG fuels as calculated by the validated model are shown. In these predictions $N = 3{,}000$ rpm and a spark timing of 25° bTDC is assumed. It is clear that cylinder pressure and work done for CNG engines are less than gasoline. In addition, the engine

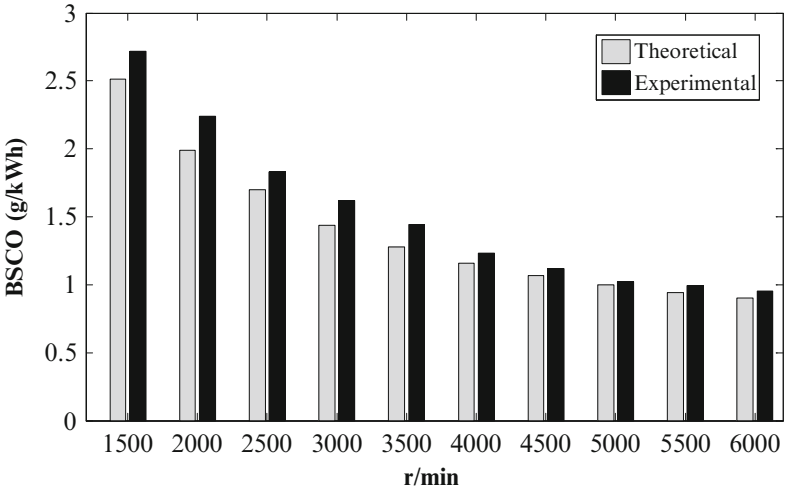

Fig. 11.7 Comparison of BSCO results (gasoline)

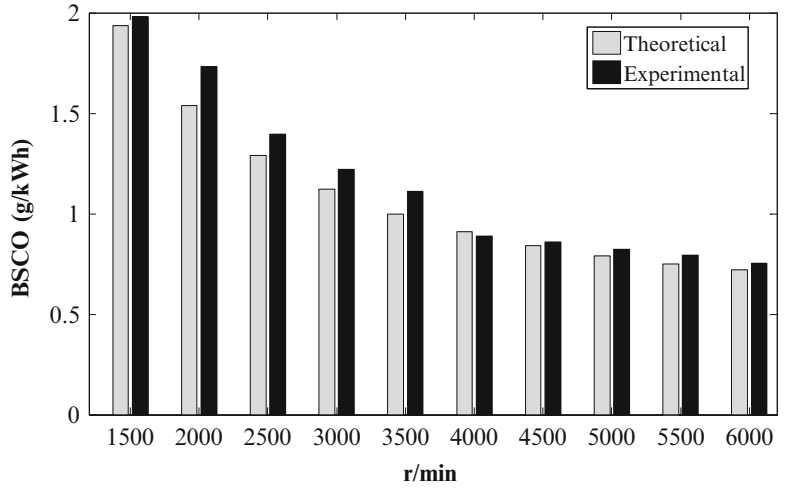

Fig. 11.8 Comparison of BSCO results (CNG)

performance in a specific engine has a high dependency on the physical condition inside the cylinder mixture.

The power produced in a specific engine has a high dependency on the physical condition of the cylinder mixture. Therefore, the volumetric efficiency performs one of the significant roles among the other engine parameters.

In Fig. 11.11, the calculated volumetric efficiency of the engine is shown at an engine speed for the gasoline and CNG fuels. Generally, the volumetric efficiency of a CNG engine is less (c.11 %) than gasoline.

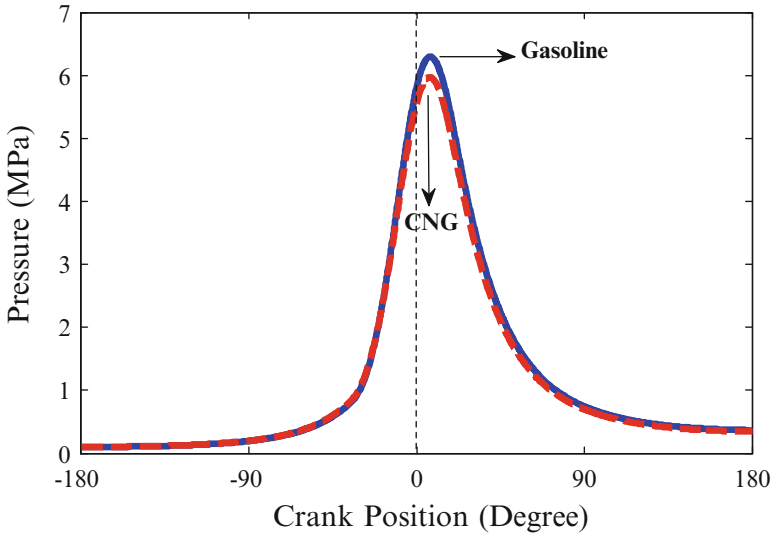

Fig. 11.9 Comparison of cylinder pressure for gasoline and CNG fuels in various crank positions

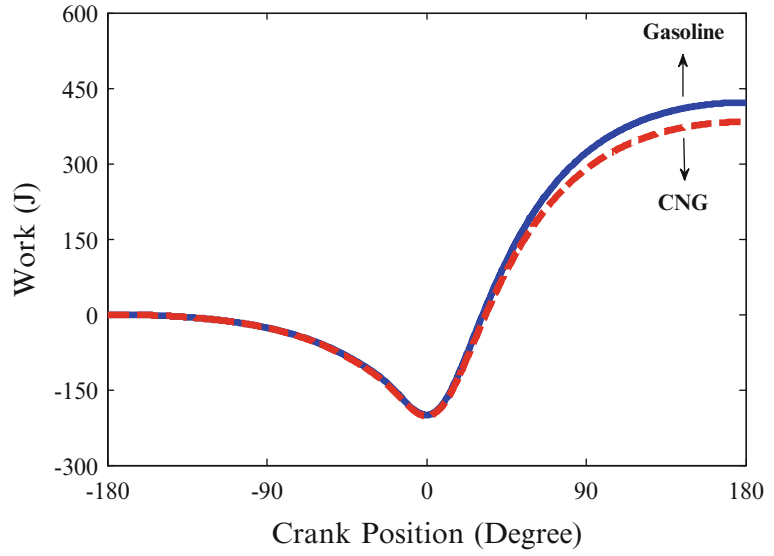

Fig. 11.10 Comparison of work done for gasoline and CNG fuels in various crank positions

This reduction in volumetric efficiency is due to two main reasons: Firstly, the vaporisation of gasoline produces a cooling effect on the intake charge. Therefore, the density of the charge is increased and the volumetric efficiency increases. Whereas with CNG, as it is already in the gaseous form at ambient vehicle

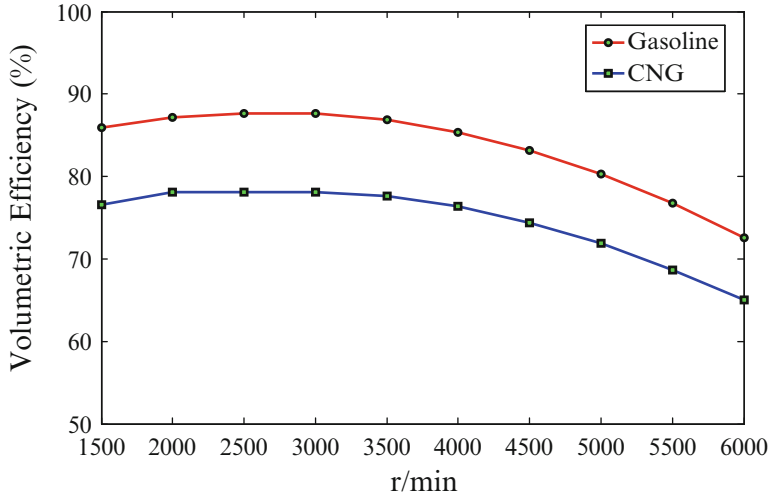

Fig. 11.11 Comparison of volumetric efficiency for gasoline and CNG fuels in various engine speeds

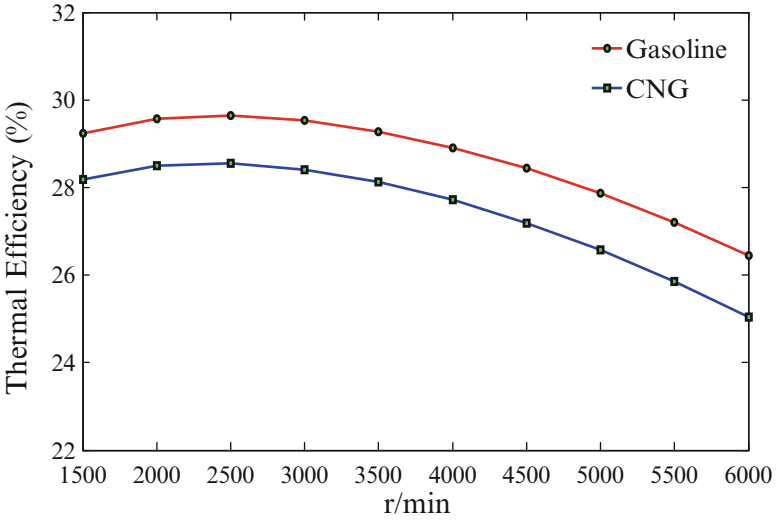

Fig. 11.12 Comparison of thermal efficiency for gasoline and CNG fuels in various engine speeds

temperatures cooling will not take place. Secondly, CNG fuel occupies a large volume in the inlet mixture; this displaces the oxygen available for combustion. These are the main reasons for a decrease in volumetric efficiency when the engine is CNG fuelled. Figure 11.12 shows that the brake thermal efficiency of a CNG engine is less (c. 4.5 %) than a gasoline-fuelled engine; hence for the CNG engine

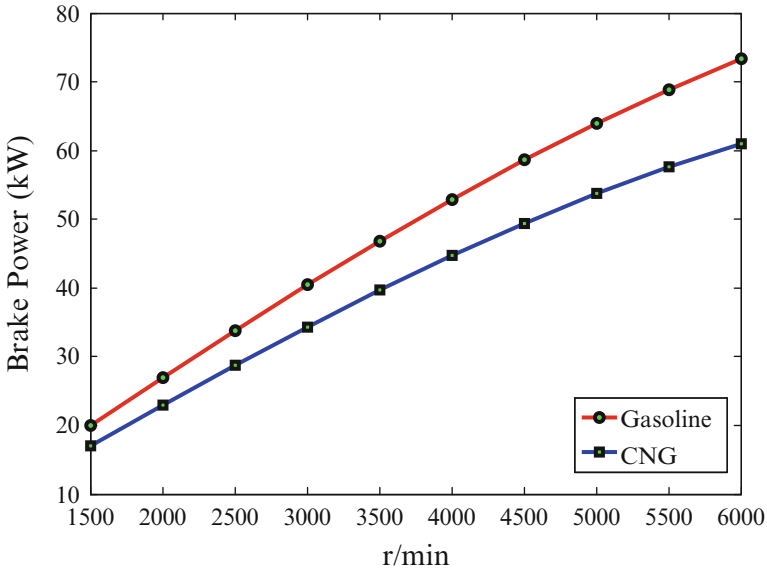

Fig. 11.13 Comparison of brake power for gasoline and CNG fuels in various engine speeds

the work produced is less even though the heating value of CNG fuel is greater than gasoline.

In Fig. 11.13, the comparative brake power (BP) of fuels is observed. As can be seen CNG produces less power (c. 15.5 %) when compared with gasoline. The reason is due to the lower volumetric efficiency of the engine when fuelled with natural gas. It should be noted that this engine has been designed for use with gasoline and not CNG. If the engine had been designed for CNG, it would have had a better performance. In order to alleviate this problem, it is possible to use turbo charging and redesign the intake manifold. Additionally the compression ratio of the engine may be increased because natural gas has a higher octane number compared with gasoline, and thus the knock limit is raised.

In Fig. 11.14, the predicted BMEP of CNG and gasoline fuels is compared. For naturally aspirated engines, the maximum BMEP is normally between 850 and 1,050 kPa [4]. As can be seen from the figure the engine BMEP when fuelled with CNG is less than gasoline by a maximum of 17 %. This reduction is due to two main reasons. Firstly, the flame speed of CNG is less than gasoline [4, 24, 25] for the same spark advance. The part of BMEP reduction happens with CNG operation that is due to longer ignition delay and lower flame speed of CNG. Therefore, the combustion should be started earlier with respect to top dead centre (TDC), and there is greater negative work done on the piston before TDC compared to gasoline. In addition, the remainder of the BMEP reduction is due to the displacement of air by CNG fuelled when the engine is gasoline base designed. Secondly, the

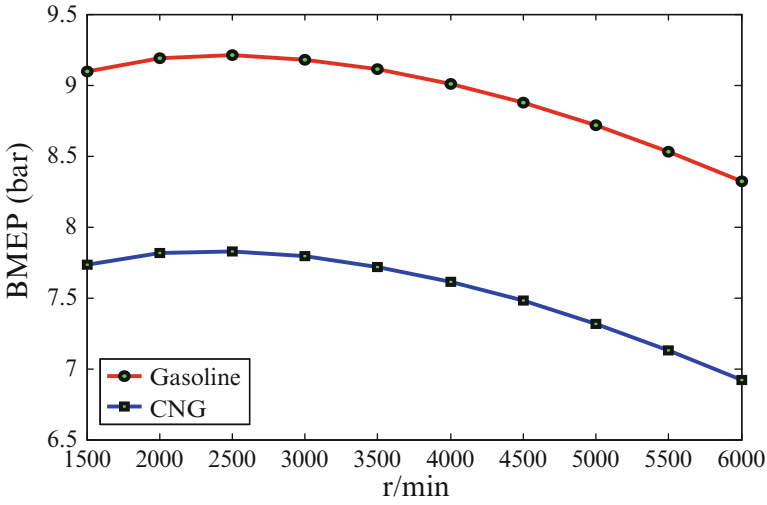

Fig. 11.14 Comparison of BMEP for gasoline and CNG fuels in various engine speeds

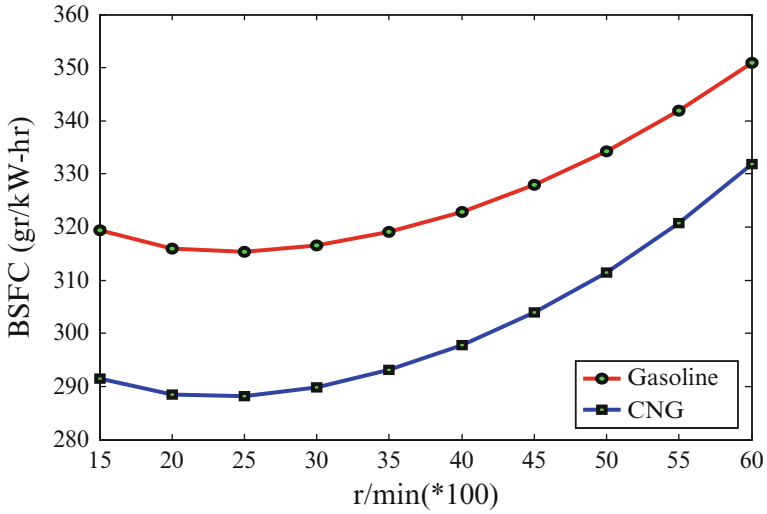

Fig. 11.15 Comparison of BSFC for gasoline and CNG fuels in various engine speeds

volumetric efficiency that plays one of the most important roles in CNG engine is less than gasoline. For these reasons, the BMEP of CNG engine is less than gasoline.

The BSFC for the fuels under study is compared in Fig. 11.15. It is obvious that the BSFC for CNG engine is less than (c. 9 %) gasoline. The main reason is the greater natural gas heating value compared to gasoline.

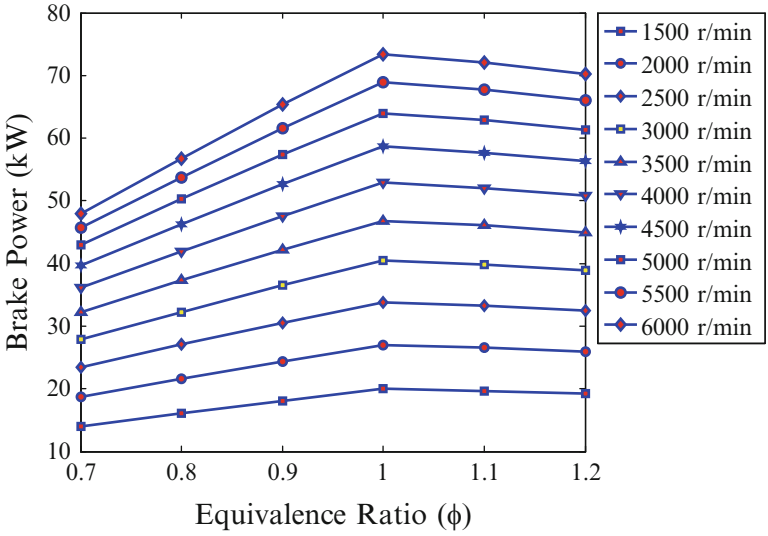

Fig. 11.16 Comparison of BP variations in various equivalence ratios (gasoline)

The equivalence ratio (ϕ) has an important effect on engine performance and emissions. Fig. 11.16 shows this effect, and it shows that brake power changes from 14 to 72 kW over the range of ϕ and speeds of the engine. Also, ϕ has a significant effect on the rate of NO_x emissions. The point of maximum NO_x emission occurs for all engine speeds at near $\phi = 0.8$; leaning or enriching the mixture from this point decreases NO_x emission rate (Fig. 11.17). However, the model predicts that CO emission is low when the mixture is lean ($\phi < 0.8$), and after $\phi > 0.8$, CO emission increases (Fig. 11.18).

Figure 11.19 shows $BSNO_x$ emissions for both CNG and gasoline fuels. It is clear that more $BSNO_x$ is created by CNG fuel than gasoline. The reactions that lead to the NO_x formation take place mainly at high temperatures. As mentioned earlier, the effect of cooling at the time of evaporation does not occur for CNG. Consequently, the initial temperature of CNG air/fuel charge at the start of combustion will be greater than gasoline.

This will lead to the increase of the maximum temperature in cylinder and finally produce more NO_x. On the other hands, with regard to the fact that the flame speed of CNG is less than gasoline, there will be a need to have a greater spark advance as compared to gasoline. The greater spark advance will increase the maximum temperature and pressure inside the cylinder. Three-way catalytic converters are used in vehicle emission control system and can be used to treat NO_x reduction specifically with the CNG operation ($0.91 < \phi < 0.95$). In addition, natural gas contains very little sulphur oxide rate (10 PPM) and for this reason has the lowest destructive effect to catalytic converters compared with gasoline [2].

In Figs. 11.20 and 11.21, the concentration of CO_2 and BSCO in exhaust gases may be observed. The amount of CO_2 in hydrocarbon combustion is proportional to

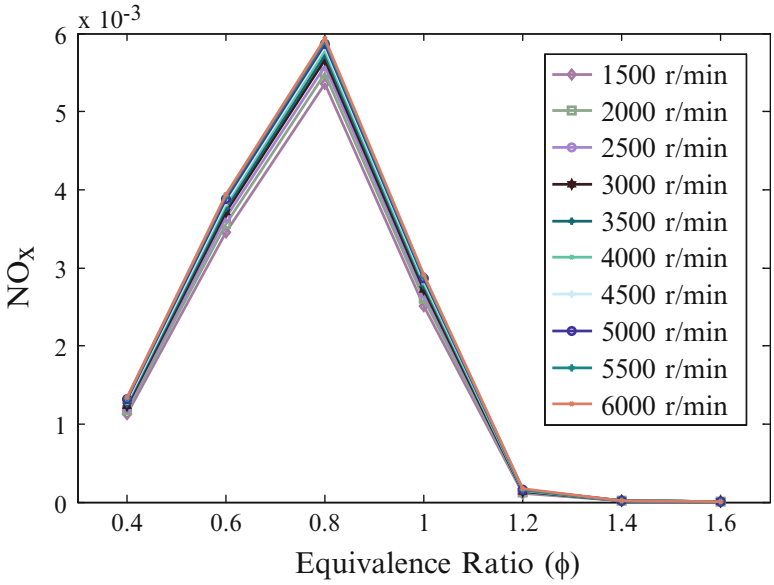

Fig. 11.17 Comparison of NO_x mole fraction in various equivalence ratios (gasoline)

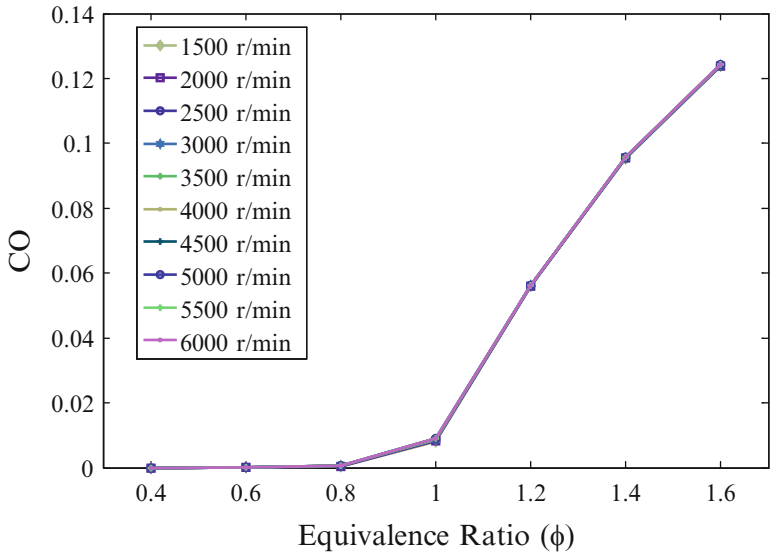

Fig. 11.18 Comparison of CO mole fraction in various equivalence ratios (gasoline)

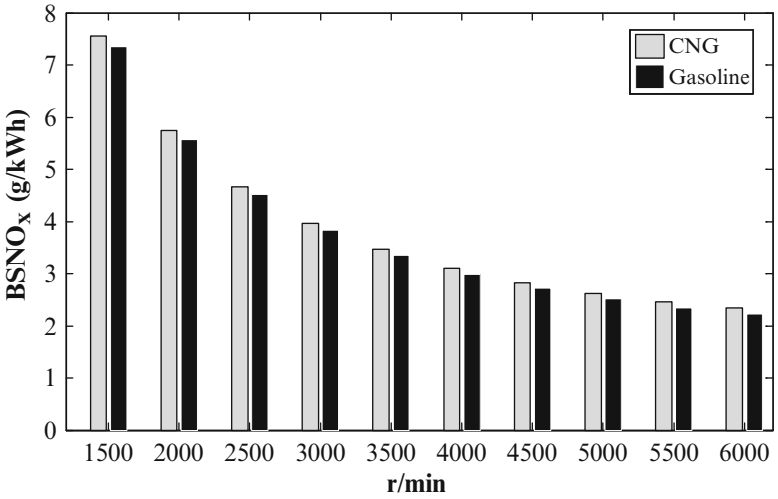

Fig. 11.19 Comparison of $BSNO_x$ for gasoline and CNG fuels in various engine speeds

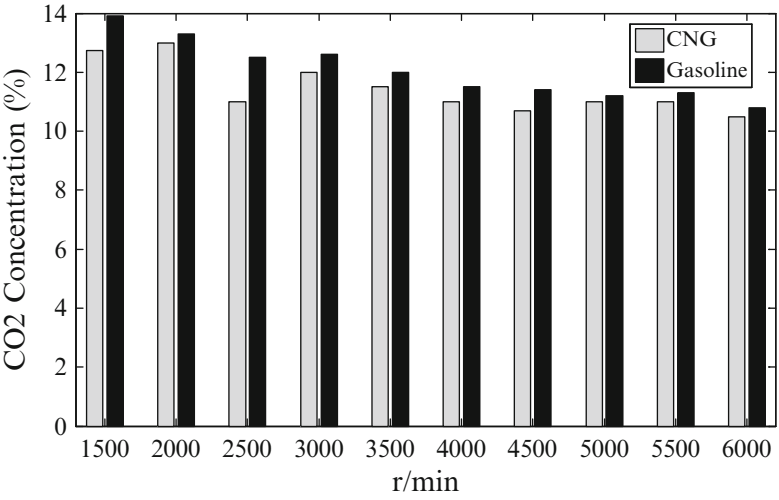

Fig. 11.20 Comparison of CO_2 concentration for gasoline and CNG fuels in various engine speeds

the carbon-to-hydrogen ratio. The main component of natural gas is methane, which has the lowest carbon-to-hydrogen ratio (C/H ratio) compared to other hydrocarbons. Therefore, the CO_2 produced in CNG combustion is less than gasoline (Fig. 11.20).

The corresponding of CO_2, C/H ratio of fuel has affecting the production of CO, for this main reason CO produced in CNG combustion less than gasoline

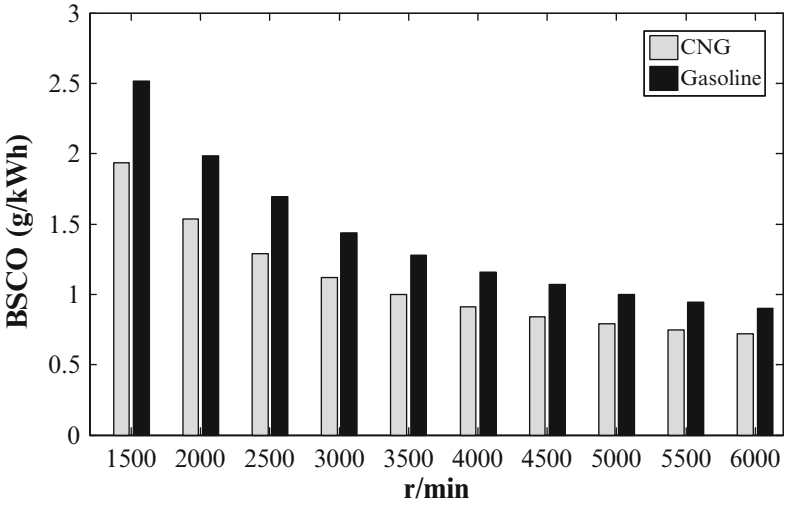

Fig. 11.21 Comparison of BSCO for gasoline and CNG fuels in various engine speeds

(Fig. 11.21). In addition, flame quenching at the walls of the cylinder and the wall oil film deposits are additional sources of CO.

Finally, as a significant result, this case study has shown that average rate reductions of CO_2 and CO for CNG engine compared to gasoline are about 29 g/km and 8 g/km [2, 23, 25], respectively. With the assumption of mean travel through the distance of each vehicle about 30,000 km (that almost are taxi), annual rate reduction of CO_2 and CO for each CNG engine will be about 860 kg/year and 240 kg/year, respectively, compared to gasoline engine.

11.5 Conclusions

A quasi-dimensional thermodynamic model of bi-fuel (CNG and gasoline) spark ignition engine was developed. It was able to simulate turbulent combustion and compared to CFD it is computationally faster and efficient. The results of the model were compared to experimental data and the validity of the model was confirmed. Therefore, this model was capable of prediction, analysis and useful for optimisation of the engine performance parameters.

In this chapter CNG was presented as an alternative fuel; it has advantages and disadvantages compared to gasoline when the engine is gasoline base designed (midterm approach).

Natural gas has smaller C/H ratio in comparison to gasoline and for this main reason it produces lower amounts of CO_2 and CO. These emissions reduction are significant annually when the vehicles specifically used such as taxi in the big city.

CNG fuel decreases volumetric efficiency, increases temperature of combustion, and finally produces more $BSNO_x$ when compared to gasoline. However, three-way catalytic converter is a part of vehicle emission control system and can treat NO_x reduction specifically with the CNG operation ($0.91 < \phi < 0.95$). Moreover, natural gas in this study contains very little sulphur oxide and for this reason has a lower destructive effect upon catalytic converters as compared to gasoline. In addition, it is cheaper than gasoline and therefore it is economic fuel. The BSFC of an engine fuelled with CNG is less than gasoline fuelled and the main reason is the greater heating value of natural gas compared to gasoline.

The volumetric efficiency plays the most important role between the other engine parameters; that is, the decreasing of volumetric efficiency in CNG will decrease the BMEP and finally decrease the work done. Therefore, the thermal efficiency of a CNG-fuelled engine is less than gasoline. Using CNG will decrease brake power (BP) in gasoline base engine designed. In order to remove this problem it is possible to use turbo charger, redesign intake manifold and increase the compression ratio.

In order to obtain an engine with less pollution, better performance and the result of this chapter, engines should be designed specifically for each type of fuel. Therefore, in the bi-fuel engine, the optimality of the performance parameters should be sacrificed.

References

1. Cho HM, He BQ (2007) Spark ignition natural gas engines-a review. J Energy Conversion Manage 48-608-618
2. Rezapour K, Ebrahimi KM (2007) The necessity of using CNG fuel and gasification of vehicle in Iran. Proceeding of 3rd international energy, exergy and environment symposium (IEEES3)
3. Lapetz J, McCarthny D, Greenfield N, Czapski R, Geftos T, Rosson J (1996) Development of the Ford QVM CNG Bi-Fuel 4.9L F-Series Pickup Truck. Society of Automotive Engineering. Paper No. 960850
4. Duan SY (1996) Using natural gas in engines: laboratory experience with the use of natural gas fuel in IC engine. IMechE Seminar Publication 39–46
5. Zuo C, Zhao KA (1997) Quasi-dimensional model of si natural gas engines with pre-chamber. Society of Automotive Engineers. Paper No. 972994
6. Evan RL, Blaszczyk JA (1997) Comparative Study of The Performance and Exhaust Emissions of a Spark Ignition Engine Fuelled by Natural Gas and Gasoline. Proc. Inst. Mech. Engrs., D00295
7. Sun X, Lutz A, Vermiglio E, Arold M, Wiedmann T (1998) The development of the GM 2.2 CNG Bi-fuel passenger cars. Society of Automotive Engineers. Paper No.982445
8. Valpato O, Theunissen F, Mazara R (2005) Engine management for multi fuel plus compressed natural gas vehicles. Society of Automotive Engineers. Paper Series 2005-01-3777
9. Alsam MU, Masjuki HH, Kalam MA, Abdessalam H, Mahlia TMI, Amalina MA (2006) An experimental investigation of CNG as an alternative fuel for a retrofitted gasoline vehicle. J Fuel Res Fuel 85:717
10. Gordon S, McBride BJ (1971) Computer program for calculation of complex chemical equilibrium composition, rocket performance, incident and reflected shocks, and Chapman Jouguet detonations. NASA publication, SP-273

11. JANAF Thermo-Chemical Tables (1971) United States National Bureau of Standard Publication, NSRDS-NBS 37
12. Ferguson CR (1968) Internal combustion engines, applied thermo-sciences. John Wiley and Sons, New York
13. Cengel YA (2005) Thermodynamic an engineering approach. Fifth Edition, McGraw Hill, New York
14. Methghalchi M, Keck JC (1980) Laminar burning velocity of propane air mixture at high temperature and pressure. Combustion Flame 38:143–154
15. Gu XJ, Haq MZ, Lawes M, Woolley R (2000) Laminar burning velocity and Markstein lengths of methane-air mixtures. Combustion and Flame, 121 (pp. 41–58)
16. Verhelst S (2005) A study of the combustion in hydrogen-fuelled internal combustion engines. PhD thesis, Ghent University, Gent, Belgium
17. Boulouchos K, Steiner T, Dimopoulos P (1994) Investigation of flame speed models for flame growth during premixed engine combustion. Society of Automotive Engineers. Paper No. 940476
18. Olikara C, Borman GL (1975) Calculating properties of equilibrium combustion products with some application to I.C. engines. Society of Automotive Engineers. Paper No. 750468
19. Depcik C (2000) Open-ended thermodynamic cycle simulation. M.S. Thesis, University of Michigan, Ann Arbor
20. Woschni G (1967) A universally applicable equation for the instantaneous heat transfer coefficient in the internal combustion engine. Society of Automotive Engineers. Paper No.670931
21. Bayraktar H, Durgun O (2003) Mathematical modelling of spark ignition engine cycles. Energy Sources 25:651–666
22. Ferguson CR, Kirkpatrick AT (2001) Internal combustion engines, applied thermo science, 2nd edn. John Wiley & Sons Inc, New York
23. Rezapour K, Ebrahimi MK, Wood AS, Nikranjbar A (2010) Simulation and modelling Bi fuel engine for the improving of performance. Society of Automotive Engineers, doi: 10.4271/2010-01-2034
24. Heywood JB (1998) Internal combustion engines fundamentals. McGraw Hill, New York
25. Rezapour K (2011) Exergy based si engine model optimisation. PhD thesis, University of Bradford, The United Kingdom